Electronic Supplementary Material (ESI) for Materials Horizons.


# Electronic Supplementary Information

**Table of Contents**

**1. Materials and methods**

**Materials.** Pentaerythritol triacrylate (PETA, 99%), dopamine hydrochloride (99%), and poly(ethyleneglycol) diacrylate (Mw=700) (PEGDA700, 98%) were purchased from Sigma-Aldrich. Triethylamine (TEA, 99%), dimethyl sulfoxide (DMSO, 99%), and methyl tertiary butylether (98%) were purchased from Tianjin Yuanli Chemical Co., Ltd. Tetraethylthiuram disufide (DS, 98%), 2,2'-Azobis(2-methylpropionitrile) (AIBN, 99%), diethyl ether, gelatin (medium gel strength, 170-195 g Bloom), and iron chloride ($FeCl_3$, AR, 98%) were supplied by Aladdin Industrial Inc. 1-vinylimidazole (VI, 99%), zinc sulfate heptahydrate ($ZnSO_4.7H_2O$, 98%), cupric sulfate ($CuSO_4$, 99 %), calcium chloride ($CaCl_2$, 96%), and nickel sulfate hexahydrate ($NiSO_4.6H_2O$, 98.5 %) were purchased from Heowns Biochem Technologies LLC.

**Preparation and characterization of HB-PBAE.** The dopamine-terminated hyperbranched polymer HB-PBAE was synthesized by a modified two-step Michael addition reaction as previous reported.[1] Briefly, PETA (10 mmol), PEGDA 700 (15 mmol), dopamine hydrochloride (36 mmol) was added to DMSO (50 mL) to fully dissolve. Herein, the molar ratio of active hydrogen to double bond was set as 1.2:1. TEA was added to the mixture to adjust a basic condition (pH=8.0). The reaction was proceeded for 2.5 hours in the dark at 80 $^oC$ under continuous stirring. Then, the reaction mixture was thoroughly washed 5 times by excess methyl tertiary butylether to remove DMSO and unreacted monomers. In the second step, dopamine hydrochloride (36 mmol in 10 mL DMSO) was added for endcapping unreacted acrylates for another 5 hours. The products were purified by excess methyl tertiary butylether, and stored in a brown vial at -20 °C.

**Preparation and characterization of HB-PBAE/Geln/PVI hydogel.** The hydrogels with various HB-PBAE concent of 0%, 5%, 10%, and 20% (w/v) was fabricated and the recipe is shown in Table S1. Typically, 33 μL of HB-PBAE (60 wt%), 100 μL of Geln (10 wt%), 17 μL of $FeCl_3$ (888 mM) and 50μL of PVI (40 wt%) were mixed together and HB-PBAE (10%)/Geln/PVI hydrogel was formed. Other hydrogels were prepared following the same process with different feed ratios.

A Rheometer (TA Instruments, Discovery, DHR-2, USA) was used to characterize the rheological properties with a 20 cm parallel-plate. Time-sweep tests were carried out at 25 $^oC$ and a frequency of 1 Hz with a strain of 1%. Frequency-sweep tests at strain = 1% were carried out at 25 $^oC$ over a frequency range from 0.6-200 rad/s. In order to observe the changes of storage modulus(G') triggered by various metal ions, 200 mM metal ion aqueous solution was added dropwise around the hydrogel when time-sweep at 300 s. The G' at 600 s was used to calculate the modulus change after 5-minute encountering metal ions.

Lap-shear tensile stress measurements of HB-PBAE/Geln/PVI hydrogels were performed using universal test machine (UTM, M350, Testometric Company Limited) and the values were calculated by dividing the maximum load by the corresponding overlapping area of each sample. Five samples for each group were used in adhesion test. A piece of pigskin after shedding off excessive fat was cut into rectangle sections at 5.0 cm × 1.5 cm. The hydrogel was injected on porcine skin and the other piece covered immediately. The overlapping area should be controlled as 1.5 cm × 1.5 cm and the samples were allowed to cure for 10 min at room temperature. A tensile tester with a 10 kgN load cell was used and the samples were fixed between the two film clamps with the tensile rate of 2 mm/min. For glass substrate, similar process

was performed using the standard glass slides with the size of 7.6 cm × 2.5 cm.

The HB-PBAE (10%)/Geln/PVI hyerogel was used to detect the effect of metal ion response on adhesion strength. The glass substrates which was coated hydrogel were separately immersed in 200 mM of metal ion solution for 10 mins, and then the adhesion strength was tested by the mothod above (n=5).

The compressive mechanical properties of hydrogels were determined by a WDW-05 electromechanical tester (Time Group Inc., China). Five samples were tested for each groups. The cylindrical hydrogel samples of 0.8 cm diameter were immersed in 200 mM metal ions aqueous solution for 2 h before test. The compression modulus was calculated by taking a strain of 0% to 10%.

The HB-PBAE hydrogel was detected by Fourier transform infrared spectrometer (FTIR, PerkinElmer spectrum 100, USA), X-ray photoelectron spectroscopy using an X-ray photoelectron spectrometer (ESCALAB 250Xi, Thermo Scientific), Scanning electron microscope (SEM, EDAX, Genesis XM2) with X-MAX20 Energy Dispersive Spectrometer (EDS), and a contact angle measuring instrument(Beijing Jinsheng Micro Technology Co., Ltd.).

**Full-thickness trauma model.** The male Sprague-Dawley (SD) rat (250±20 g) was used to construct the full-thickness trauma model.[2] The whole process of the animal experiment was carried out in accordance with the regulations and rules of the Tianjin Biomedical Engineering Institute. All procedures were approved by Animal Ethics Committee of Institute of Radiation Medicine Chinese Academy of Medical Sciences (approval number: IRM-DWLL-2018071). The back hair was removed by animal hair clippers after being anesthetized by chloral hydrate. Four full-thickness wounds of 1.6 cm in diameter were created on both sides of the spine. Ring-shaped silicone rings were secured around the wound using 6-0 nylon sutures to prevent wound contraction. The wounds were randomly divided into four groups. “PBS treatment” (PBS), “$Zn^{2+}$ solution” ($Zn^{2+}$), “HB-PBAE (10%)/Geln/PVI hydrogel alone” (HB-PBAE (10%)/Geln/PVI) and “HB-PBAE (10%)/Geln/PVI hydrogel + $Zn^{2+}$” (HB-PBAE (10%)/Geln/PVI hydrogel/$Zn^{2+}$) (n =10). For the hydrgel treated wounds, 200 μL hydrogel was injected into the wounds by 1 mL syringes. For the $Zn^{2+}$ and PBS group, 200 μL of 200 mM $ZnSO_4$ aqueous solution or PBS solution was uniformly distributed on the surface of the wound with a medical cotton swab. All wounds were covered with commercially available transparent film dressing (Tegaderm Film, 3M, MN) to prevent loss of moisture.

Wound dressing change was carried out in the 5th and 10th day. For the HB-PBAE (10%)/Geln/PVI group, the hydrogel was directly removed with tweezers and then debrided by physiological saline. For the HB-PBAE (10%)/Geln/PVI/$Zn^{2+}$ group, 200 μL of 200 mM $Zn^{2+}$ aqueous solution was sprayed on the wound before the dressing change, and then the hydrogel was peeled off with tweezers after 10 minutes. Digital photographs were taken after dressing change and the wound area was measured using Image J software (NIH, MD). The percentage of the original wound area at different time points was calculated by comparing them to the wound area on the day of surgery. 15 days after the surgery, the rats were sacrificed by overdosed anaesthetic, then the granulation tissues were harvested and fixed with 4 % paraformaldehyde for 48 hours, and dehydrated in a graded series of ethanol, and then embedded in paraffin for routine

hematoxylin-eosin (H&E) staining and Masson's-trichrome staining. The stained sections were observed and recorded by an OLYMPUS CKX41 microscope (OLYMPUS, Japan).

**Statistical analysis.** All data in the experiment were expressed as mean ± standard deviation. Data analyses were performed using the SPSS 17.0 software. Statistical analysis was assessed by the independent sample ANOVA test. The differences were considered statistically significant at the value of $p < 0.05$.

**2. Supplementary Tables.**

**Table S1.** The formula of hydrogels with different ratios.

| Samples | HB-PBAE (wt%) | PVI (wt%) | Geln (wt%) | $FeCl_3.6H_2O$ (mM) |
|---|---|---|---|---|
| Geln | 0 | 10 | 5 | 75 |
| HB-PBAE (5%)/Geln/PVI | 5 | 10 | 5 | 75 |
| HB-PBAE (10%)/Geln/PVI | 10 | 10 | 5 | 75 |
| HB-PBAE (20%)/Geln/PVI | 20 | 10 | 5 | 75 |

**Table S2.** FTIR major peak positions and assignments for PVI.

| Peak position ($cm^{-1}$) | Assignment |
|---|---|
| 1663 | υ(C=C,C=N) (ring) |
| 1497 | υ(C=C,C=N) (ring) |
| 1418 | $\upsilon$(ring)+$\delta_s(CH_2)$ (backbone) |
| 1285 | β(CH) (ring)+υ(C=N) (ring) |
| 1228 | β(CH) (ring)+υ(C=N) (ring) |
| 1111 | β(CH) (ring) |
| 1085 | β(CH) (ring)+υ(ring) |

**Table S3.** The wound healing rate by various treatments.

| Group | Day 5 | Day 10 | Day 15 |
|---|---|---|---|
| HB-PBAE (10%)/Geln/PVI | 18.0±2.0 | 37.0±2.6 | 82.7±1.5 |
| Urgo | 15.2±1.0 | 39.3±0.8 | 82.0±1.0 |

The Urgo dressing was purchased from Urgo Medical as a commercial comparison. The main ingredients of Urgo are guar gum, galactose, mannose and propylene glycol. As revealed by the quantitative evaluation of the wound healing rate in Table S3, the healing rate of HB-PBAE/Geln/PVI/$Zn^{2+}$ group shows no significantly difference in the wound closure rate with that of Urgo dressing.

**Table S4.** The swelling rates of the HB-PBAE (10%)/Geln/PVI hydrogels.

| | $H_2O$ | $Ca^{2+}$ | $Cu^{2+}$ | $Ni^{2+}$ | $Zn^{2+}$ |
|---|---|---|---|---|---|
| 0 min | 100.0 | 100.0 | 100.0 | 100.0 | 100.0 |
| 5 min | 113.1±1.2 | 109.1±2.7 | 106.7±1.0 | 105.3±0.4 | 104.0±1.3 |
| 10 min | 123.9±1.3 | 116.5±2.3 | 111.9±0.1 | 109.3±0.5 | 105.8±1.3 |
| 20 min | 128.9±1.0 | 122.4±0.9 | 115.2±0.1 | 111.8±0.1 | 107.0±1.4 |
| 40 min | 133.7±1.0 | 127.3±1.4 | 118.3±0.2 | 108.5±6.0 | 108.5±0.8 |
| 1 h | 157.8±1.9 | 132.1±2.1 | 120.8±1.3 | 114.0±0.0 | 110.2±1.7 |
| 3 h | 166.7±2.2 | 160.0±3.1 | 125.8±1.1 | 121.5±0.1 | 115.9±2.7 |
| 5 h | 172.3±1.1 | 167.5±3.1 | 129.0±1.4 | 125.1±1.6 | 120.5±2.9 |
| 7 h | 176.9±0.7 | 172.5±3.7 | 134.6±2.0 | 129.3±1.7 | 123.7±1.7 |
| 9 h | 177.4±1.9 | 172.8±3.3 | 138.1±2.0 | 131.3±2.8 | 126.0±1.7 |

The hydrogels show a distinct swelling ratio after soaking in $Ca^{2+}$, indicating a weak interaction between $Ca^{2+}$ and polymer chains in the hydrogel. However, the hydrogels do illustrate a much less remarkable change on swell ratio after soaking in $Cu^{2+}$, $Ni^{2+}$, and $Zn^{2+}$ solution. The complexation of imidazole groups and metal ions will increase the crosslinking density of the hydrogel and make the hydrogel network more compact to inhibit water swelling.

**3. Supplementary Figures.**

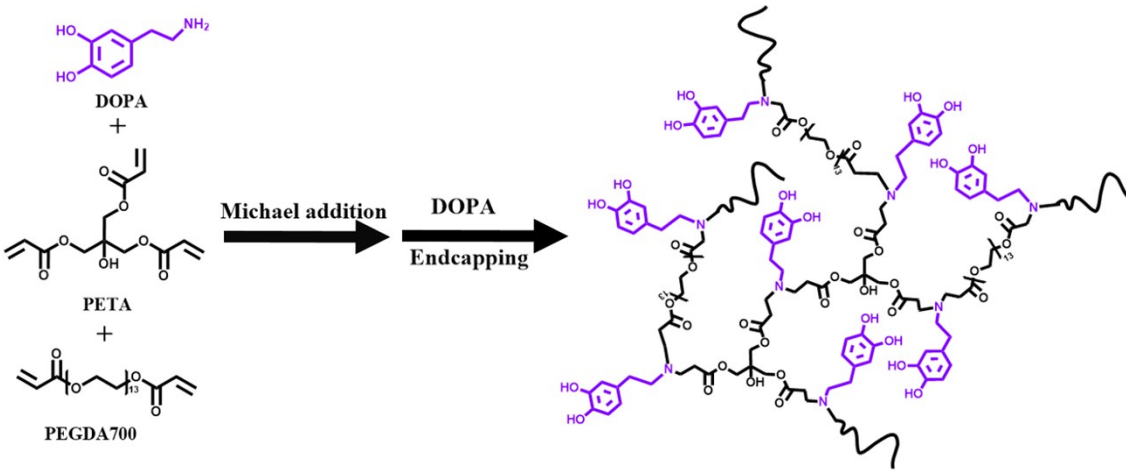


**Figure S1.** Chemical synthesis of HB-PBAE.

The HB-PBAE was synthesized by two-step Michael addition reaction between amino and double bond and the resulted hyperbranched polymer was end-capped with DOPA.

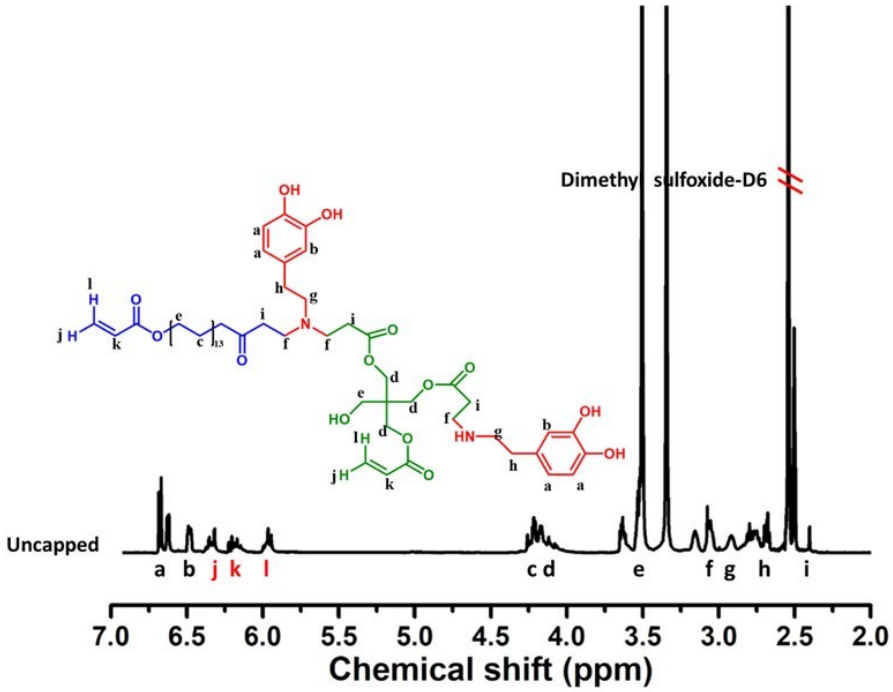


**Figure S2.** $^{1}$H NMR spectrum of HB-PBAE before end-capping.

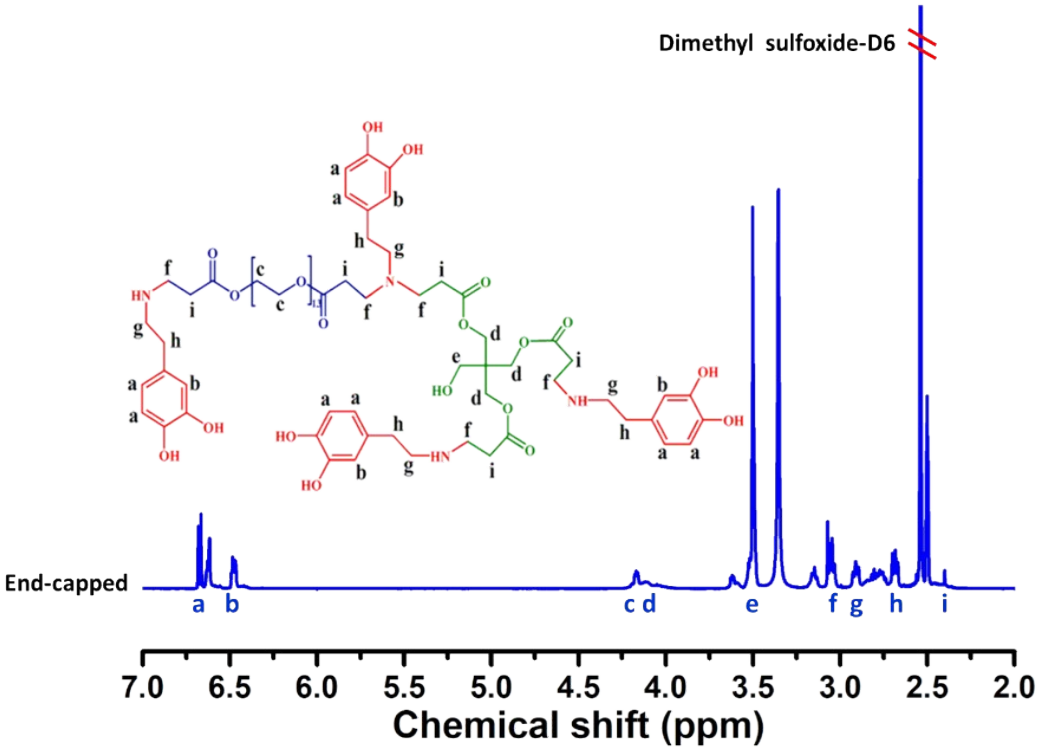


**Figure S3.** $^{1}$H NMR spectrum of HB-PBAE after end-capping.

$^{1}$H NMR spectroscopy of HB-PBAE was carried out a nuclear magnetic resonance spectrometer ($^{1}$H-NMR, 500 MHz, Varian INOVA) and used Dimethyl sulfoxide-D6 to lock the chemical shifts. As shown in Figure S2 and S3, the proton peaks at 6.6 ppm and 6.4 ppm attributed to catechol group can be found in the $^{1}$H NMR spectra of uncapped and end-capped HB-PBAE. However, the proton peaks of acrylate at 6.2 ppm, 6.3 ppm, and 6.0 ppm appear only in $^{1}$H NMR spectra of uncapped HB-PBAE, suggesting a complete end-capping.

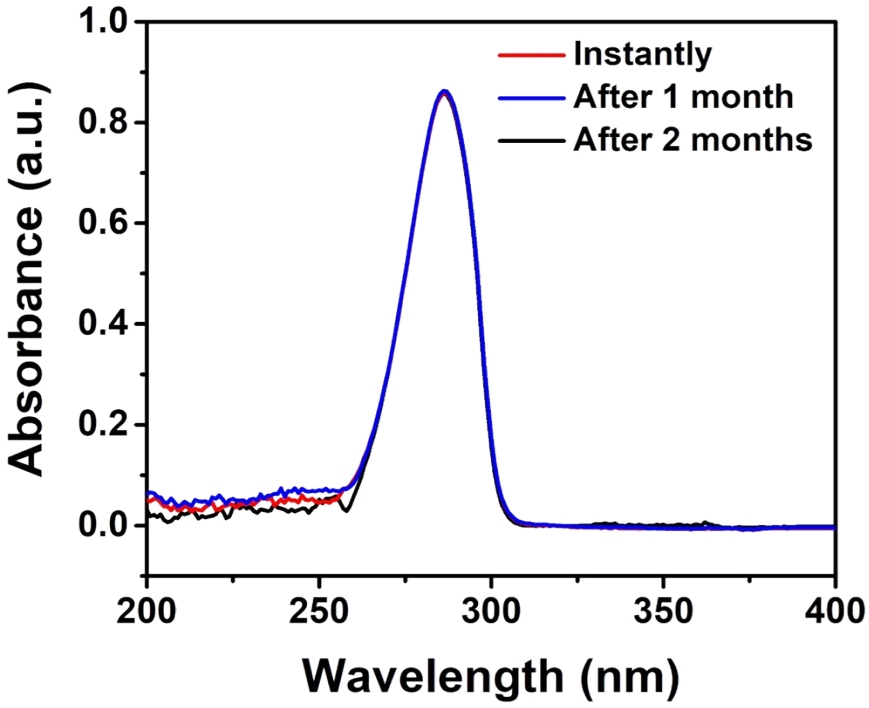


**Figure S4.** UV-Vis absorption spectra of HB-PBAE solution.

UV-Vis absorption spectra of HB-PBAE solution (0.25 mg/mL) in DMSO at room temperature under air atmosphere was tracked for instantly, a month and two months using a UV-Vis spectrometer (TU-1810 DPC, China). Characteristic absorption peak of catechol groups at 280 nm was distinctly observed and remained changeless for 2 months, indicating the catechol groups kept unoxidized.

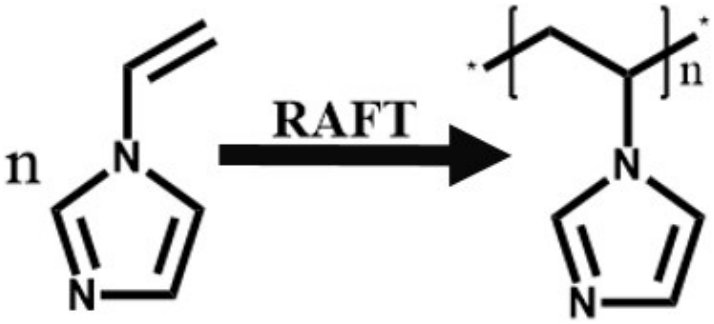


**Figure S5.** Chemical synthesis of PVI.

The PVI was synthesized by the RAFT reaction, using AIBN as an initiator and DS as a chain transfer agent. Briefly, VI (62.5 mmol), DS (1.25 mmol), AIBN (2.5 mmol), DMF (25 mL) was thoroughly mixed in a round bottom flask, especially the molar ratio of DS, AIBN and VI was 1:2:50. Then the reaction was carried out at 70°C for 6.5 h in a nitrogen atmosphere. In addition, the reaction mixture was cooled to room temperature, and purified by diethyl ether for 5 times. The final product was stored at -20 $^{o}$C.

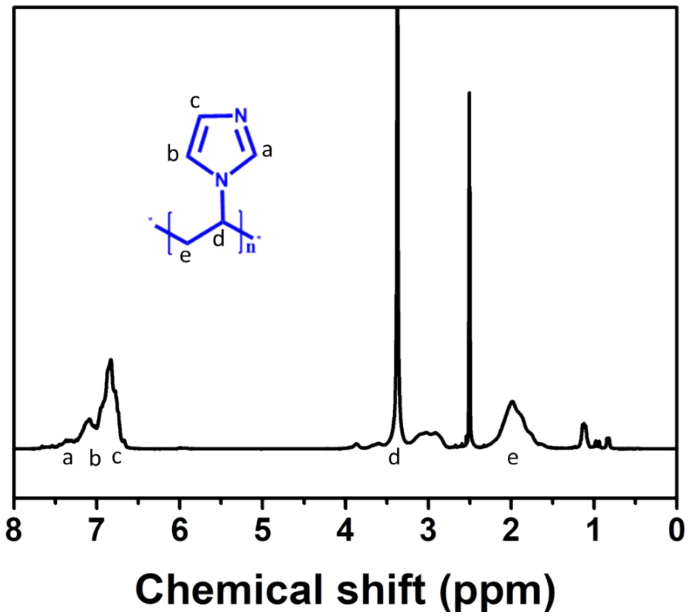


**Figure S6.** $^{1}$H NMR spectrum of PVI.

The broad peak of about 7 ppm was the proton peak on the imidazole ring after VI polymerization, the proton peaks on the double bonds of VI at 5.3 ppm was absent, indicating that VI has been successfully polymerized.

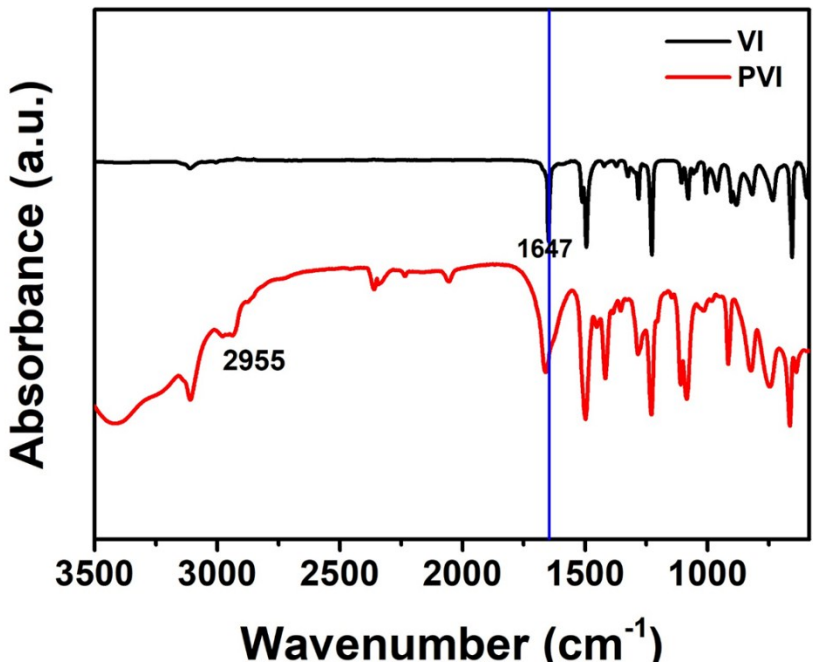


**Figure S7.** FT-IR spectra of VI and PVI.

Infrared Spectrometry was performed using Fourier transform infrared (FTIR, PerkinElmer spectrum 100, USA). As shown in Figure S7, the characteristic absorption bands of imidazole ring can be seen at 3108, 1497, 1284, 1083, 744, 633 $cm^{-1}$. The peak representing the C=C double bond at 1647 $cm^{-1}$ disappeared in the infrared spectrum of PVI, and the characteristic peaks of CH and $CH_2$ at 2935-2965 $cm^{-1}$ appeared on PVI, indicating that PVI has been successfully synthesized.

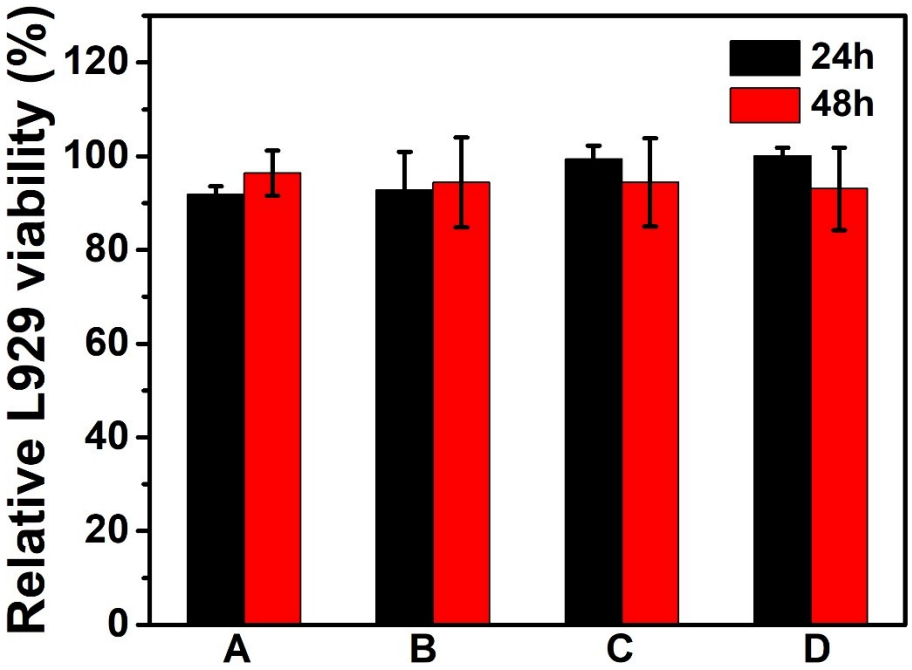


**Figure S8.** Relative L929 cell viability of samples using hydrogel extracts after incubation for 24 and 48 hours. A: HB-PBAE (0%)/Geln/PVI; B: HB-PBAE (5%)/Geln/PVI; C: HB-PBAE (10%)/Geln/PVI; D: HB-PBAE (20%)/Geln/PVI.

Cytotoxicity was evaluated by determining the viability of L929 mouse fibroblasts exposed to the hydrogel extracts using quantitative MTT assay. Figure S8 indicated L929 cells remained a favorable viability of >90% for all groups, suggesting the hydrogels had good biocompatibility.

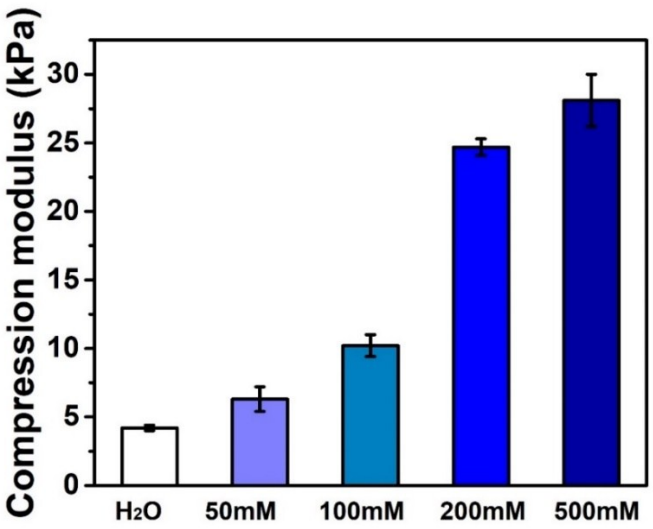


**Figure S9.** Compression modulus of HB-PBAE (10%)/Geln/PVI hydrogels after complexed by different concentrations of zinc ion solution for 10 minutes.

As shown in Figure S9, the compressive modulus of the hydrogels increases with the concentration of zinc ions. The compressive modulus was 24.7 kPa when the concentration was 200 mM, which was 2.4 times as that of the hydrogels soaking in 100 mM $ZnSO_4$. Comparing the modulus at 200 mM zinc ions, the modulus only increases 1.1 times as that of the hydrogels soaking in 500 mM $ZnSO_4$. Based on these results, a zinc ion solution with a concentration of 200 mM was chosen for further research.

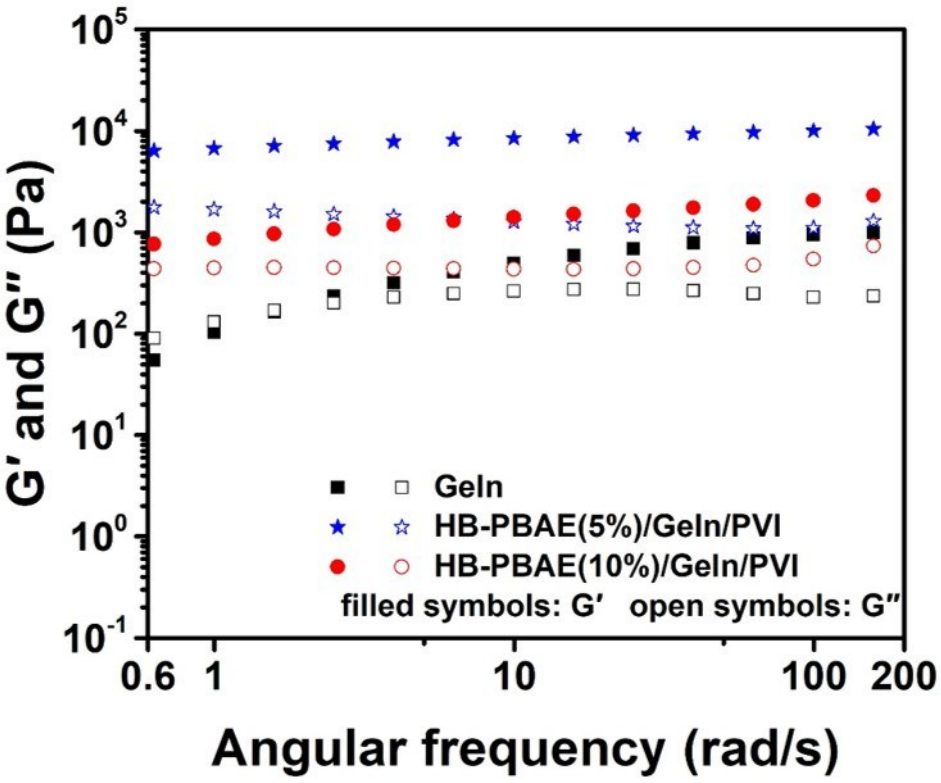


**Figure S10.** The frequency-scan curves of the hydrogels.

A Rheometer (TA Instruments, Discovery, DHR-2, USA) was used to study the rheological properties with a 20 cm parallel-plate. Frequency-sweep tests at strain = 1% were carried out at 25 $^{o}$C over a frequency range from 0.6-200 rad/s.

As represented in Figure S10, except for the GeIn group which is a viscous sol at low frequencies, all other groups, G′ is dominant over G′′ within the angular frequency from 0.6 to 200 rad/s, indicating that the hydrogels were stable and behaved as a viscoelastic solid.

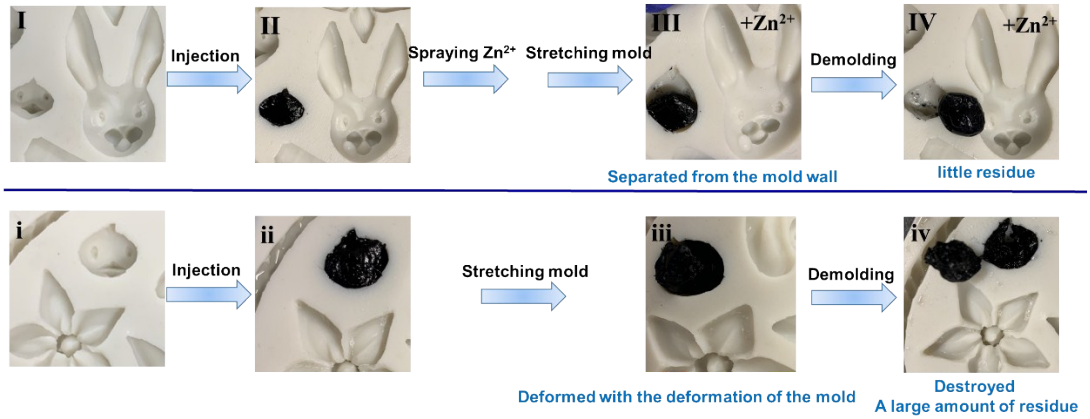


**Figure S11.** The photographs showing demolding process of the separation of HB-PBAE (10%)/Geln/PVI hydrogels from the complex mold; I, i) The complex molds; II, ii) The HB-PBAE (10%)/Geln/PVI hydrogels were injected into the molds; III, iii) Photographs showing HB-PBAE (10%)/Geln/PVI hydrogels after the stretching of molds; IV, iv) Photographs indicating the HB-PBAE (10%)/Geln/PVI hydrogel demolded by the stretching molds.

As shown in Figure S11, HB-PBAE (10%)/Geln/PVI hydrogels were injected into a complex mold for rapid prototyping. After the hydrogels were completely cured, 200 mM $Zn^{2+}$ aqueous solution was sprayed. Then the mold was pulled as shown in Figure S11 III and iii, the $Zn^{2+}$- responsiveness hydrogel could be swiftly separated from the mold wall, while the hydrogel in absence of zinc ions still sticks tightly to the mold. As shown in Figure S11 IV and iv, the hydrogels after spraying $Zn^{2+}$ can be completely separated from the mold with very little residue, while the hydrogel in absence of zinc ions is broken in parts during the demolding process with a large amount of hydrogel residue in the mold. Therefore, the HB-PBAE (10%)/Geln/PVI hydrogels possess not only a good injectability to fill irregular wounds but also a convenient demolding capability after spraying zinc ions.

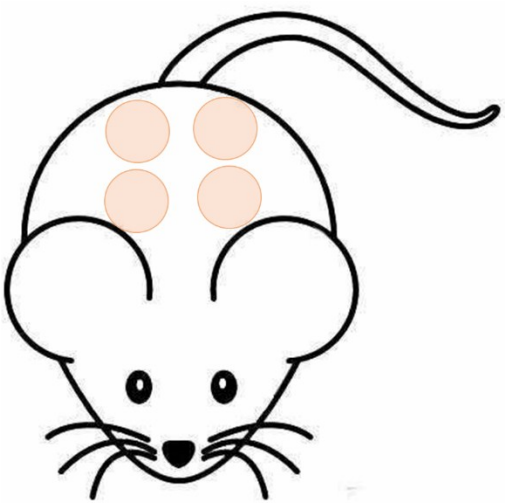

**Figure S12.** Schematic diagram of rat wound bed administration. Four wounds were randomly assigned to PBS, $Zn^{2+}$, HB-PBAE (10%)/Geln/PVI, and HB-PBAE (10%)/Geln/PVI/$Zn^{2+}$.

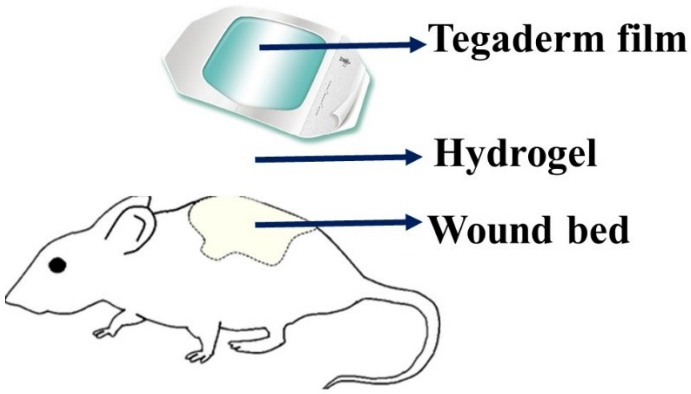


**Figure S13.** Schematic diagram to illustrate the position of our hydrogel and Tegaderm film.

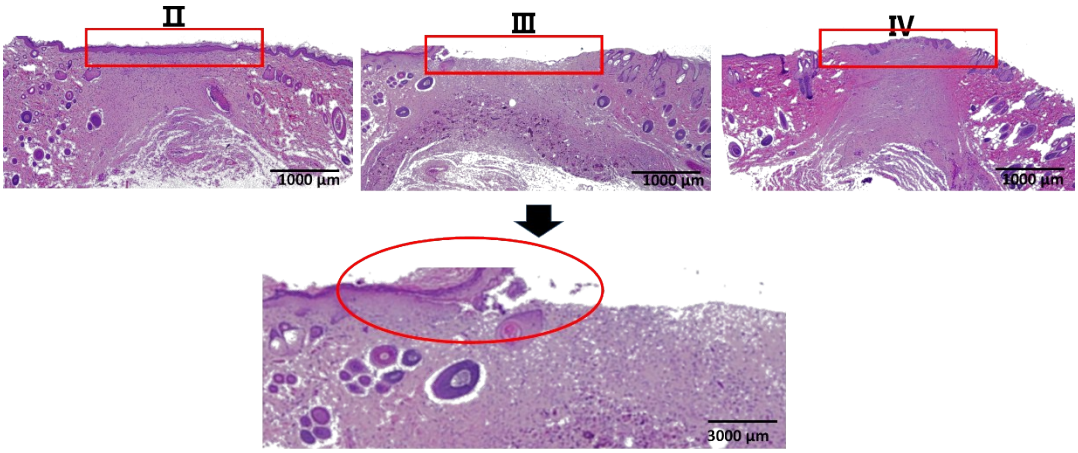


**Figure S14.** The tissue surrounding the defects was excised and stained by H&E at day 15. (II: $Zn^{2+}$; III: HB-PBAE (10%)/Geln/PVI; IV: HB-PBAE (10%)/Geln/PVI/$Zn^{2+}$).

The epithelial layer of the HB-PBAE (10%)/Geln/PVI group was incomplete and the collagen fibers were disorderly arranged, indicating that the skin integrity was significantly impaired.

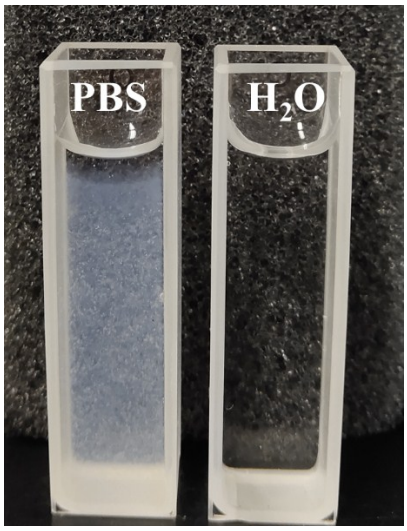


**Figure S15.** Photographs of $ZnSO_4$ solution in PBS and water.

As shown in Figure S15, a flocculant of zinc hydroxide is formed in 200 mM $ZnSO_4$ / PBS solution (pH = 7.4). Based on this outcome, the $Zn^{2+}$ / water solution is chosen rather than $Zn^{2+}$ / PBS solution.

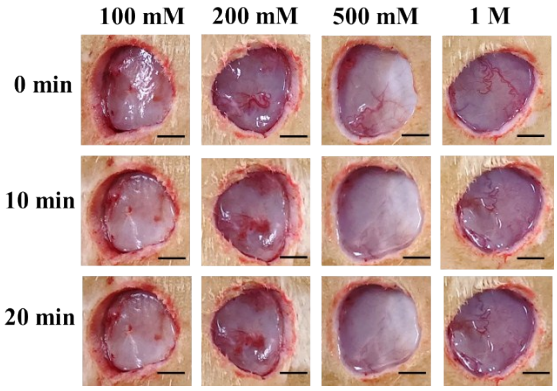


**Figure S16.** Photographs of different concentrations of zinc ions added to rat wound beds. Scale bar: 0.5 cm.

Four full-thickness wounds of 1.6 cm in diameter were created on both sides of the rat spine. Then 200 μL of 100 mM, 200 mM, 500 mM, and 1 M $ZnSO_4$ aqueous solution was uniformly distributed on the surface of the wound beds with a medical cotton swab separately. As shown in Figure S16, there was no abnormal redness after different concentrations of zinc ions were added to wound beds within 20 min, indicating that the zinc ion solution was not irritating.


**Figure S17.** Schematic diagram of impact force calculation by water flow.

200 μL of the HB-PBAE (10%)/Geln/PVI hydrogel was adhered to the pigskin, and then 200 μL of 200 mM Zinc ion aqueous solution was added dropwise to the hydrogel. After 10 minutes, the hydrogel was tested at different velocity of flow (Figure S17). The impact force when the hydrogel was washed away by the water flow was calculated to be 0.14 N by Formula S1.

$$F = Q\rho v \quad \text{S1}$$

Where F, Q, ρ, v are impact force, flow, density, and flow rate, respectively.

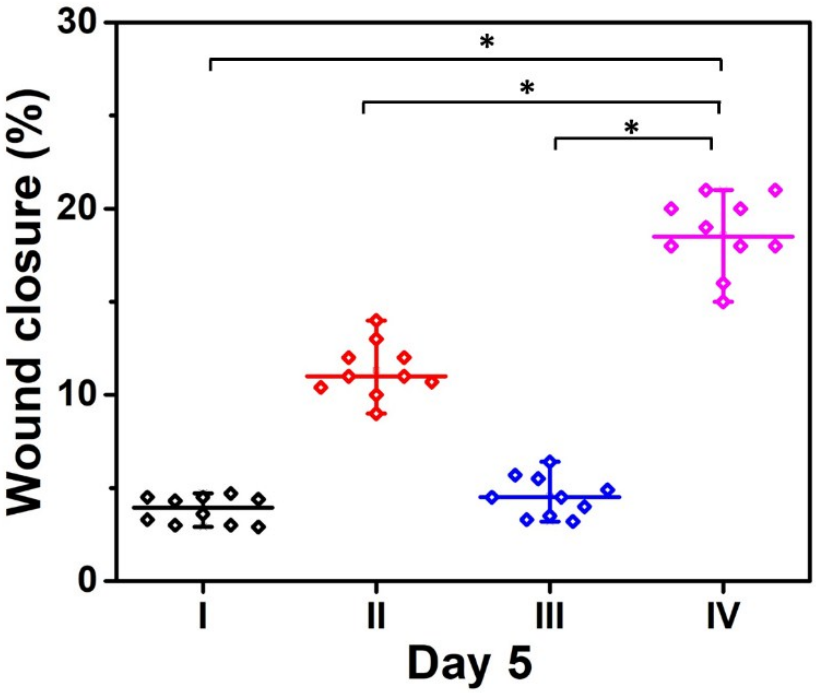


**Figure S18.** Wound healing rate by various treatments on the 5th day.

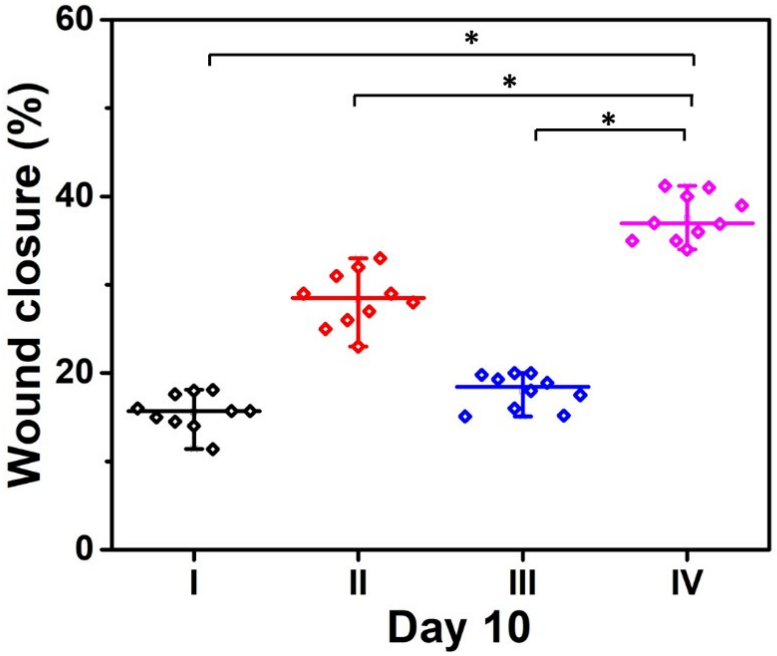


**Figure S19.** Wound healing rate by various treatments on the 10th day.

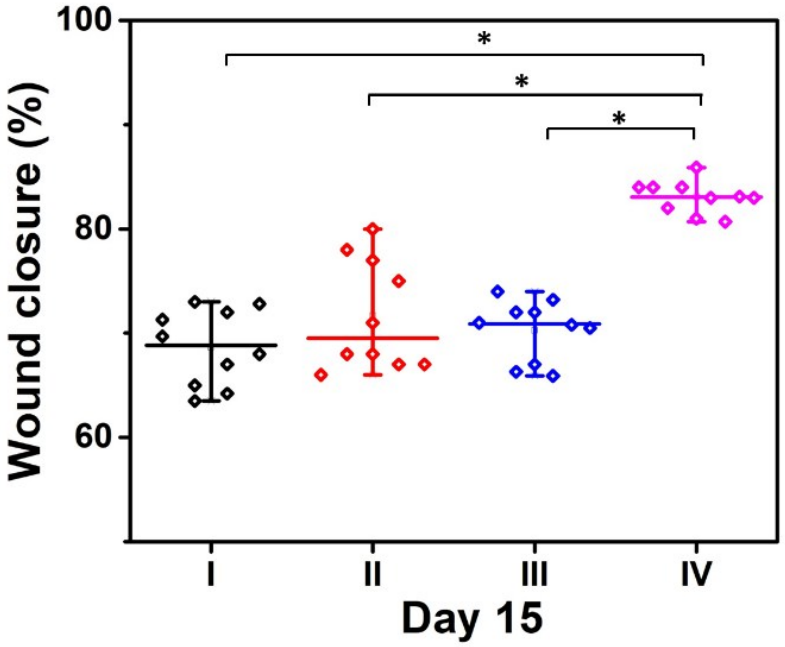


**Figure S20.** Wound healing rate by various treatments on the 15th day.

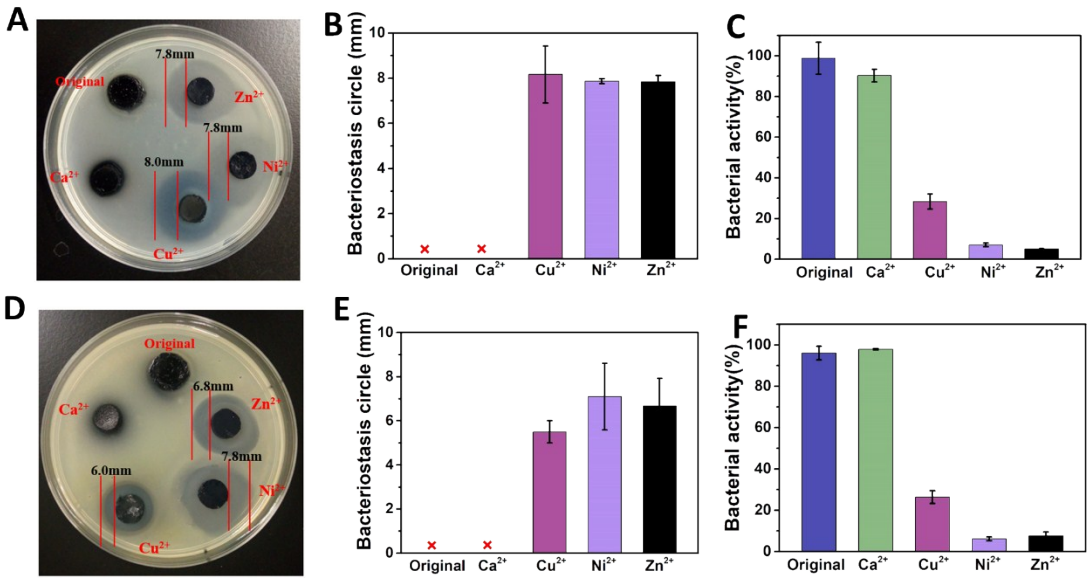


**Figure S21.** Antimicrobial activities of the hydrogel treated by metal ions by disc diffusion assay (A, B, D, E) and suspension assay (C, F) for S. aureus (Gram-positive bacterium) (A, B, C) and E. coli (Gram-negative bacterium) (D, E, F). Bacterial-only solution was used as a control and the relative bacterial viability (mean ± SD, n = 3) was expressed as $Abs_{sample}/Abs_{control}$× 100%.

Original hydrogel and treated by $Ca^{2+}$ shows no antibacterial activity against either S. aureus or E. coli, significant bacteriostasis circles appeared in the remaining components. And the antibacterial ring sizes of S. aureus and E. coli treated with $Cu^{2+}$, $Ni^{2+}$ and $Zn^{2+}$ were 8.2 mm, 7.9 mm, 7.8 mm and 5.5 mm, 7.1 mm, 6.7 mm, respectively. The suspension assays also showed that the bacterial killing efficiency of S. aureus and E. coli about hydrogel which treated by $Cu^{2+}$, $Ni^{2+}$ and $Zn^{2+}$ was above 70%.[3] Therefore, it has been confirmed that a hydrogel treated with $Cu^{2+}$, $Ni^{2+}$ and $Zn^{2+}$ has an outstanding antibacterial effect.

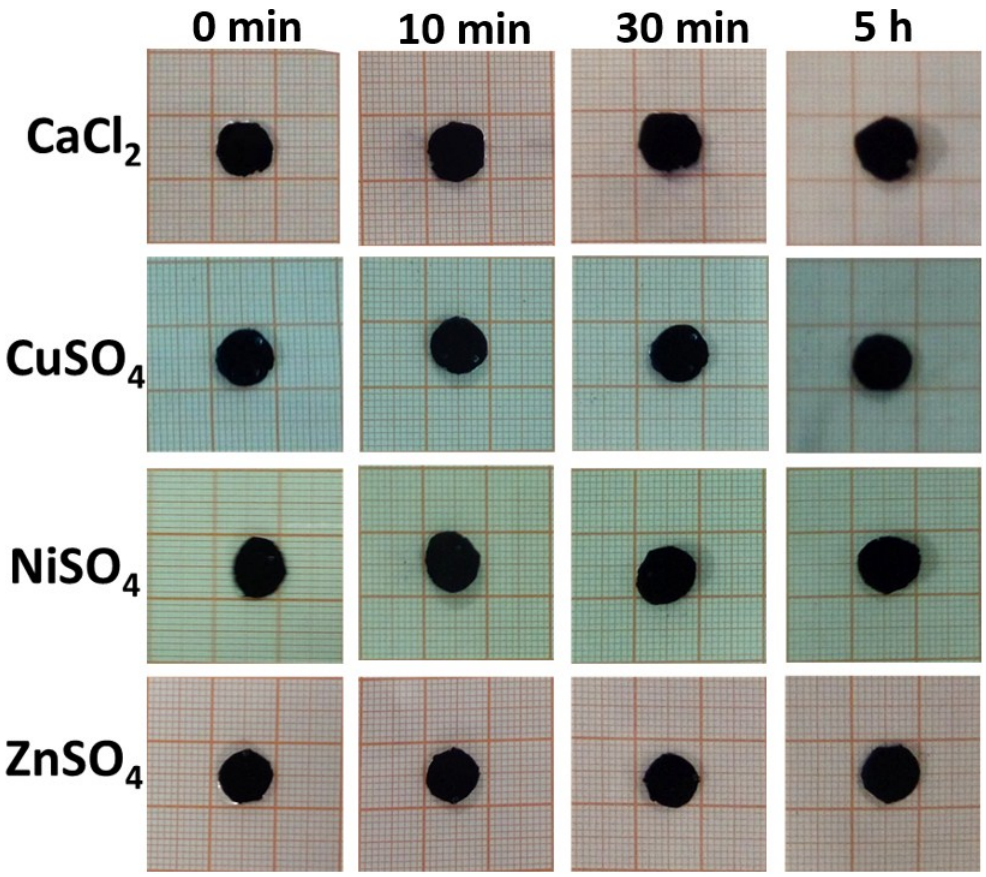


**Figure S22.** The volume monitoring of HB-PBAE (10%)/Geln/PVI was immersed in200 mM $Ca^{2+}$, $Cu^{2+}$, $Ni^{2+}$, $Zn^{2+}$ aqueous solution for 0 min, 10 min, 30 min and 5 h respectively.

It can be seen from the Figure S22 that the hydrogel of the soaked $Ca^{2+}$ aqueous solution was slightly expanded, and the other groups were not aware of much change. There are two main opposites. On the one hand, the complexation of the imidazole ring and the metal ion increases the crosslink density of the hydrogel and makes the hydrogel network more compact. On the other hand, the metal ion solution is slightly acidic due to its hydrolysis, and under acidic conditions, the imidazole ring undergoes protonation and the hydrogel network swells. These two opposite effects cancel each other out, so there is no significant change in the volume of the hydrogel.[4]

**4. References**


1 H. Zhang, L. P. Bre, T. Y. Zhao, Y. Zheng, B. Newland and W. X. Wang, *Biomaterials*, 2014, **35**, 711.

2 R. D. Galiano, J. Michaels, M. Dobryansky, J. P. Levine and G. C. Gurtner, *Wound Repair Regen.*, 2004, **12**, 485.

3 J. F. Song, P. F. Zhang, L. Cheng, Y. Liao, B. Xu, R. Bao, W. Wang and W. G. Liu, *J. Mater. Chem. B*, 2015, **3**, 4231.

4 A. Horta, M. J. Molina, M. R. Gómez-Antón and I. F. Piérola, *Macromolecules*, 2009, **42**,1285.